Res Chem Intermed
DOI 10.1007/s11164-014-1591-z

Synthesis and optical properties of two cationic cyclopentadienyliron complexes of arene containing the triphenylbutene structure

Tao Wang · Jiqiang Liu · Junru Han · Guanglei Li · Xiaoning Wang

Received: 13 December 2013 / Accepted: 11 March 2014

Abstract Two novel cationic cyclopentadienyliron complexes of arene containing the triphenylbutene group (TPBE-Fc) were synthesized and characterized by IR, UV–visible, ^{1}H NMR, and ^{13}C NMR spectroscopy, and by MS. The optical properties of the compounds were studied by experimental and theoretical methods. Positive solvatochromism of the UV–visible absorption of TPBE-Fc on increasing the solvent polarity was observed experimentally. Quantum chemical calculations of the orbital energy, geometric structure, absorption spectra, and first hyperpolarizability (β) values of the TPBE-Fc were performed by use of density functional (DFT/B3LYP and TD-DFT) methods. The spectra observed experimentally were in good agreement with the calculated values. The calculated HOMO and LUMO energies revealed the presence in the compounds of charge transfer mediated by the metal center.

Keywords Triphenyl conjugated butene · Synthesis · Cyclopentadienyliron · Optical property · Quantum chemical calculation

---

T. Wang (✉)
State Key Laboratory of Chemical Resource Engineering, College of Science, Beijing University of Chemical Technology, Beijing 100029, People's Republic of China
e-mail: wangtwj2000@163.com

J. Liu · J. Han
Department of Organic Chemistry, College of Science, Beijing University of Chemical Technology, Beijing 100029, People's Republic of China

G. Li
Beijing Schengenbiya Bioengineering Technology Company Limited, Beijing 100029, People's Republic of China

X. Wang
College of Material Engineering, Beijing Institute of Fashion Technology, Beijing 100019, People's Republic of China

Introduction

The electron-donating and electron-accepting capabilities of organic–ligand–metal species have been successfully used in push–pull substituted chromophores to obtain special functional molecules. Recent studies have shown that this kind of organic material has promising features for use in optical devices [1–8]. Stilbene-containing and triphenylbutene-containing π-conjugated compounds are particularly promising classes of organic nonlinear materials. Research has shown that these kinds of organic material have large second-order optical nonlinearity and might be good candidates for electro-optic modulators [9–11]. Stilbene-containing π-conjugated compounds containing a metallic atom in their structures have the combined properties of the metal and the stilbene [12–16].

Stilbene-containing and triphenylbutene-containing π-conjugated compounds containing ferrocenyl groups have been reported to have special biological and medicinal activity [17–21].

In this paper we report the synthesis, characterization, and optical properties of two novel D-π-A cyclopentadienyliron complexes of arene containing the triphenylbutene structure (TPBE-Fc). TPBE-Fc contain a push–pull system formed by diphenyl ether or diphenyl sulfide as donor group and cationic cyclopentadienyliron as acceptor group. Quantum chemical calculations of the orbital energy, geometric structure, absorption spectra, and first hyperpolarizability (β) for TPBE-Fc were performed by use of density functional (DFT/B3LYP and TD-DFT) methods.

Experimental

Materials and instruments

All chemicals used were of analytical reagent grade from commercial sources and used without further purification. (η^6-Chlorobenzene) (η^5-cyclopentadienyl) iron hexafluorophosphate (Fc-Cl) was prepared by ligand-exchange reaction of ferrocene and chlorobenzene as described elsewhere [22, 23].

^{1}H NMR and ^{13}C NMR spectra were recorded on a Bruker 400 high resolution console, using d_6-acetone as deuterated solvent and TMS as internal standard. FT-IR spectra were recorded on a Nicolet 5700 instrument (Thermo Electron Corporation, Waltham, MA, USA). UV–visible absorption spectra were recorded on an Hitachi U2500 spectrophotometer (Hitachi High-Technologies, Tokyo, Japan). Fluorescence spectra were obtained on an Hitachi F-4500 spectrophotometer at room temperature. Elemental analysis was performed with Thermo–Finnigan Flash EA 1112 CHNS/O analyzer.

Computational details

In this work we used density functional theory (DFT) at the Becke 3-Lee–Yang–Parr (B3LYP)/Genecp [24, 25] (Fe with Lanl2dz basis set [26] and C, H, N, and O with 6-31G** basic set [27, 28]) basis set level for computation of the molecular structures and energies of the optimized structures in the ground state. All calculations were performed by use of Gaussian09 software [29]. The absorption spectra of TPBE-Fc were calculated by use of the time-dependent density functional theory (TD-DFT) method from gas phase optimized geometries [30, 31].

The dipole moment (μ), mean polarizability (α), and total first static hyperpolarizability (β) of TPBE-Fc were calculated in terms of x, y, z components, which are given by the equations:

$$\mu = \left(\mu_x^2 + \mu_y^2 + \mu_z^2\right)^{1/2} \tag{1}$$

$$\alpha = \left(\alpha_{xx} + \alpha_{yy} + \alpha_{zz}\right)/3 \tag{2}$$

$$\begin{aligned} \beta &= \left(\beta_x^2 + \beta_y^2 + \beta_z^2\right)^{1/2} \\ \beta_j &= \beta_{jjj} + \sum\left(\beta_{jii} + 2\beta_{ijj}\right)\Big/3 \quad (i \neq j; i,j = x,y,z) \end{aligned} \tag{3}$$

The β components of the Gaussian output are reported as atomic units and, therefore, the calculated β components have been converted into electrostatic units β_{tot} (esu) (1 *a.u.* = 8.6393×10^{-33} esu) [32, 33].

General methods for preparation of hydroxy-substituted triphenylbutene (TPBE) and TPBE-Fc

The experimental procedure used in this study was based on that used in our previous study [21]. The synthetic route to TPBE-Fc is shown in Scheme 1. Ketones were prepared by acylation of diphenyl ether and diphenyl sulfide. TPBE were then prepared from the ketones by McMurry coupling with hydroxybenzophenone, with Zn and $TiCl_4$ as catalysts. The reaction was easy to perform and gave good yields of mixtures of *Z* and *E* isomers. TPBE-Fc were then synthesized by S_NAr reaction of the TPBE with Fc-Cl in *N*,*N*′-dimethylformamide (DMF), in the presence of potassium carbonate as base, at 80 °C. Completion of the S_NAr reaction was monitored by observing the disappearance of Fc-Cl by thin-layer chromatography with acetone–methanol (1:1) as mobile phase and Silica gel as stationary phase.

Characterization data for 1-(4-Hydroxyphenyl)-1-phenyl-2-(4-phenyloxyphenyl)butene (TPBE-1)

Yield: 68.2 %, *Z/E* isomers ratio of 4:3. m.p. = 87–90 °C. ^{1}H NMR (400 MHz, acetone-d_6) δppm: 0.88–0.94 and 1.15–1.21 (2 × t, 3H, $-CH_3$), 2.40–2.46(q, 2H, $-CH_2-$), 8.16 and 8.37 (2 × s, 1H, –OH), 6.43–7.28 (m, 18H, Ar). ^{13}C NMR (100 MHz, acetone-d_6) δppm: ((157.85, 157.49) *C*–OH), ((155.51, 155.20, 154.60, 153.79) *C*–O–*C*), ((141.21, 140.43, 138.57, 137.58, 135.89, 135.51, 131.08, 130.89, 127.38, 127.02, 125.72, 122.98, 119.03, 118.54, 117.69, 117.27, 115.05, 114.41, 113.98,) *Ph, C*=*C*), ((29.21, 28.92) $\mathit{C}H_2CH_3$), ((13.92, 13.71) $CH_2\mathit{C}H_3$). FT-IR (KBr cm^{-1}): 3347.3 (m, O–H), 2974.7 (m, $-CH_3$), 2873.4 (m, $-CH_2-$), 1699.1 (w, –C=C–), 1222.1 (s, C–O). ESI–MS (*m/z*): 393 $[M + 1]^+$.

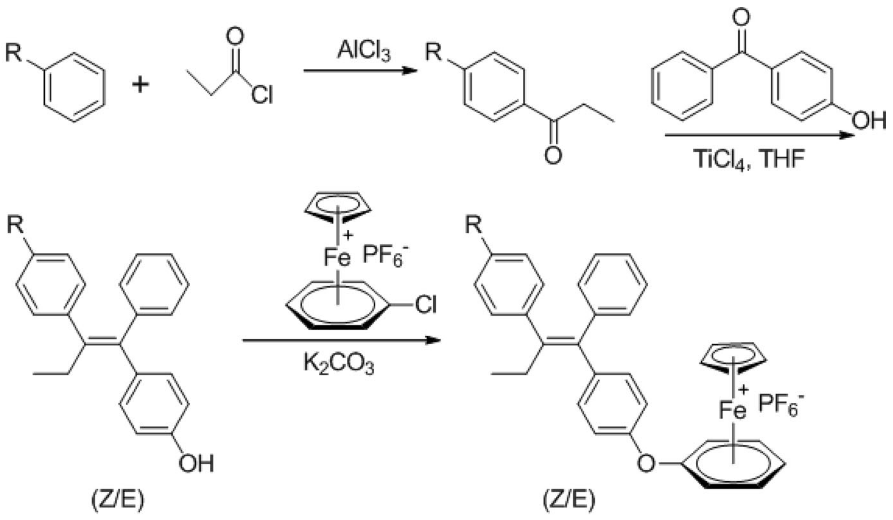

TPBE

TPBE-1 R = -PhO

TPBE-2 R = -PhS

TPBE-Fc

TPBE-Fc-1 R = -PhO

TPBE-Fc-2 R = -PhS

Scheme 1 Synthesis of TPBE-Fc

Characterization data of 1-(4-Hydroxyphenyl)-1-phenyl-2-(4-phenylthiophenyl)butene (TPBE-2)

Yield: 50.8 %, *Z/E* isomers ratio of 4:1. m.p. = 92–95 °C. ^{1}H NMR (400 MHz, acetone-d_6) δppm: 0.84–0.90 and 1.12–1.19 (2 × t, 3H, –CH_3), 2.38–2.45(q, 2H, –CH_2–), 9.23 and 9.44 (2 × s, 1H, –OH), 6.40–7.26 (m, 18H, Ar); ^{13}C NMR (100 MHz, acetone-d_6) δppm: ((153.41, 152.66) *C*–OH), ((142.66, 142.45, 139.88, 139.58, 135.79, 135.52, 134.61, 134.38, 131.09, 130.19, 129.81, 129.63, 128.81, 128.04, 126.35, 125.91, 125.53, 124.83, 113.99, 113.36) *Ph, C–S–C, C=C*), ((28.02, 27.71) *C*H_2CH_3), ((12.91, 12.61) CH_2*C*H_3). FT-IR (KBr cm^{-1}): 3383.1 (m, –OH), 2953.9 (m, –CH_3), 2867.4 (m, –CH_2–), 1696.1 (w, –C=C–), 1219.2 (s, C–O), 1168.5 (s, C–S). ESI–MS (*m/z*): 409 $[M + 1]^+$.

Characterization data of [(η^5-Cyclopentadienyl)-Fe-(η^6-(1-(4-phenoxyphenyl)-1-phenyl-2- (4-phenoxyphenyl) butene] hexafluorophosphate (TPBE-Fc-1)

Yield: 59.1 %, *Z/E* isomers ratio of 3:2. m.p. = 106–108 °C. ^{1}H NMR (400 MHz, acetone-d_6) δppm: 0.89–0.93 (2 × t, 3H, –CH_3–), 2.39–2.56 (q, 2H, –CH_2–), 5.09 and 5.18 (2 × s, 5H, Cp), 6.02–6.20 (m, 5H, Ar), 6.76–7.42 (m, 18H, Ar). ^{13}C NMR (100 MHz, acetone-d_6) δppm: ((157.31, 157.08, 156.92, 155.68, 155.59, 155.48, 150.90, 150.55) *C–O–C*), ((142.77, 142.00, 137.01, 136.83, 133.52, 133.21, 130.98, 129.56, 126.12, 125.58, 123.30, 123.08, 119.99, 119.45, 118.74, 118.61, 118.55, 118.49) *Ph, C=C*), ((87.71, 87.47, 86.09, 85.65) *Ph*(*C, C*)-Fe-Cp), ((77.84, 77.66) *Ph*(*C*)-Fe-Cp), ((77.04, 76.73) Ph-Fe-*Cp*(*C*)), ((29.26, 28.99,) CH_2CH_3), ((13.73, 13.56) CH_2CH_3). FT-IR (KBr cm^{-1}): 2942.3 (m, $–CH_3$), 2864.5 (m, $–CH_2–$), 1234.1 (s, C–O), 831.7 (s, P–F). ESI–MS (*m/z*): 589[M-145(PF_6^-)]$^+$. Anal. Calc. for $C_{39}H_{34}F_6FeO_2P$ (590.5 g mol^{-1}): C, 79.32; H, 5.80; O, 5.42. Found: C, 79.01; H, 5.78; O, 5.31.

Characterization data of [(η^5-Cyclopentadienyl)-Fe-(η^6-(1-(4-phenoxyphenyl)-1-phenyl-2- (4-phenylthiophenyl) butene] hexafluorophosphate (TPBE-Fc-2)

Yield: 60.6 %, *Z/E* isomers ratio of 4:1. m.p. = 125–128 °C. ^{1}H NMR (400 MHz, acetone-d_6) δppm: 0.90–0.96 (2 × t, 3H, $–CH_3–$), 2.41–2.58 (q, 2H, $–CH_2–$), 5.10 and 5.19 (2 × s, 5H, Cp), 6.14–6.35 (m, 5H, Ar), 6.92–7.47 (m, 18H, Ar); ^{13}C NMR (100 MHz, acetone-d_6) δppm: ((151.89, 150.89, 142.14, 141.78, 140.90, 140.42, 137.95, 137.64, 135.32, 135.08, 133.58, 131.12, 130.86, 130.56, 130.22, 129.71, 129.44, 128.42, 126.53, 126.17, 120.42, 120.00, 119.01, 118.67, 117.45, 117.95) *Ph, C*–O–*C, C*–S–*C, C=C*), ((86.80, 86.65, 84.87, 84.72) *Ph* (*C, C*)-Fe-Cp), ((77.02, 76.97) *Ph*(*C*)-Fe-Cp), ((76.83, 76.55) Ph-Fe-*Cp*(*C*)), ((28.22, 28.08), CH_2CH_3), ((13.34, 13.26) CH_2CH_3). FT-IR (KBr cm^{-1}): 2974.5 (m, $–CH_3$), 2874.4 (m, $–CH_2–$), 1243.1(s, C–O), 1165.5 (s, C–S), 825.7 (s, P–F). ESI–MS (*m/z*): 605 [M-145(PF_6^-)]$^+$. Anal. Calc. for $C_{39}H_{34}F_6FeOSP$ (606.1 g mol^{-1}): C, 77.22; H, 5.65; S, 5.29; O, 2.64. Found: C, 76.98; H, 5.56; S, 5.17; O, 2.51.

Results and discussion

Characterization and molecular geometry of TPBE-Fc

The chemical structure of TPBE-Fc was confirmed by IR, ^{1}H NMR, and ^{13}C NMR spectroscopy, and by MS; results are given in the "Experimental" section. The most useful diagnostic resonances in the NMR spectra of TPBE or TPBE-Fc were the singlets from the phenolic hydroxyl groups of TPBE and the cyclopentadienyl groups of TPBE-Fc. The ^{1}H NMR spectra of TPBE-Fc-1 and TPBE-Fc-2 are shown in Fig. 1. Obviously, the singlets for the phenolic hydroxyl and cyclopentadienyl groups have split into two peaks because of the *E/Z* isomerization shown in Fig. 1. For direct comparison we measured the chemical shifts and the integrals of the singlets for TPBE (~9.30 ppm) and TPBE-Fc (~5.10 ppm) in the NMR spectra. We tried to obtain the *trans* and *cis* isomers by column chromatography and fractional crystallization but could not isolate the pure isomers. Assignments in NMR spectra of *cis–trans* mixtures are tentative; peaks were, in part, identified by analogy with the work of Collins et al. [34], who used NMR chemical shifts to distinguish between *cis* and *trans* antiestrogenic and antifertility compounds. Their work showed that for substitution of the aromatic ring *trans* to the alkyl group, the *E* isomer peaks were approximately 0.1–0.2 ppm downfield of the corresponding peaks for the *Z* isomers. *E*-to-*Z* isomer ratios were estimated from the peak heights

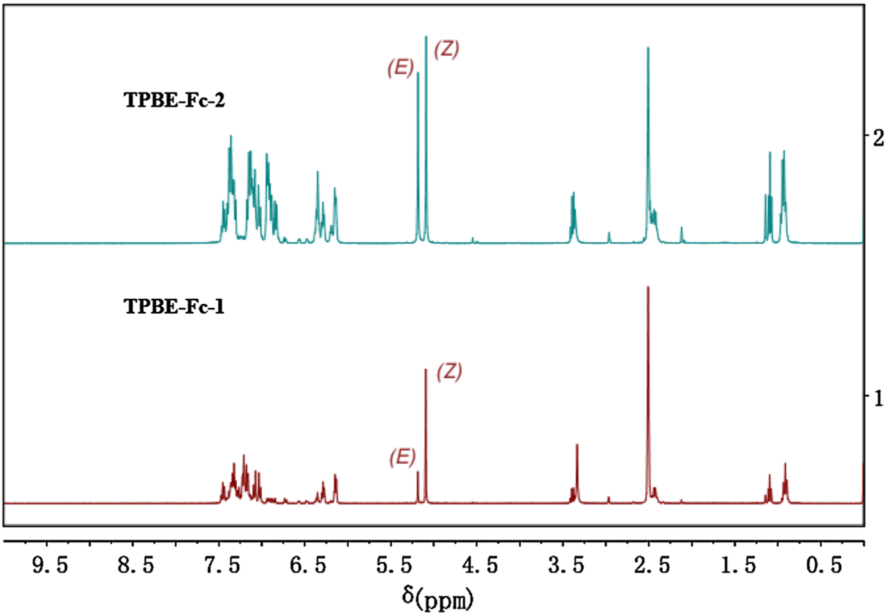

Fig. 1 ^{1}H NMR spectra of TPBE-Fc-1 and TPBE-Fc-2

of the appropriate phenolic hydroxyl group and cyclopentadienyl group resonances; the results are given in the "Experimental" section.

The geometric structure of (*E*)-TPBE-Fc, optimized at the DFT level by use of the B3lyp/Genecp(6-31G**/Lanl2dz) basis set, is shown in Fig. 2. Optimized structural data, including predicted bond lengths, valence angles, and dihedral angles, are listed in Table 1, on the basis of the atomic numbering scheme given in Fig. 2. Steric hindrance results in spatial dihedral angles among the three phenyl rings bonded with double bonds. As shown in Table 1, bond lengths and valence angles for TPBE-Fc agree with those of structures of closely related compounds determined by X-ray crystallography [35]. The C=C bond length calculated for *E*-TPBE-Fc is 1.338 Å; the reference values for *cis*-tamoxifen (*E*) and *trans*-tamoxifen (*Z*) are 1.33 Å and 1.34 Å, respectively. The angle formed by the double bond and one of the four substituents is of the order of 122°–124° for both the *cis* and *trans* tamoxifen (reference values). For (*E*)-TPBE-Fc-1 the bond angles are: C(30)–C(33)–C(45) 123.0°, C(34)–C(33)–C(45) 123.3°, C(33)–C(45)–C(57) 123.4°, and C(33)–C45)–C(47) 121.0°. For (*E*)-TPBE-Fc-2, the bond angles are: C(30)–C(33)–C(45) 123.0°, C(34)–C(33)–C(45) 123.3°, C(33)–C(45)–C(57) 123.5°, and C(33)–C45)–C(47) 121.1°. There is widening of the angle on the ethyl side and narrowing on the side on which the diphenyl ether or diphenyl sulfide group is located. This is probably attributable to the greater bulk of the cyclopentadienyl iron group, which is located at the other side of the ethylene skeleton relative to the diphenyl ether or diphenyl sulfide group. It is also apparent that the four substituents on the double bond do not lie in the same plane, the C(47)–C(45)–C(33)–C(30) atoms forming a

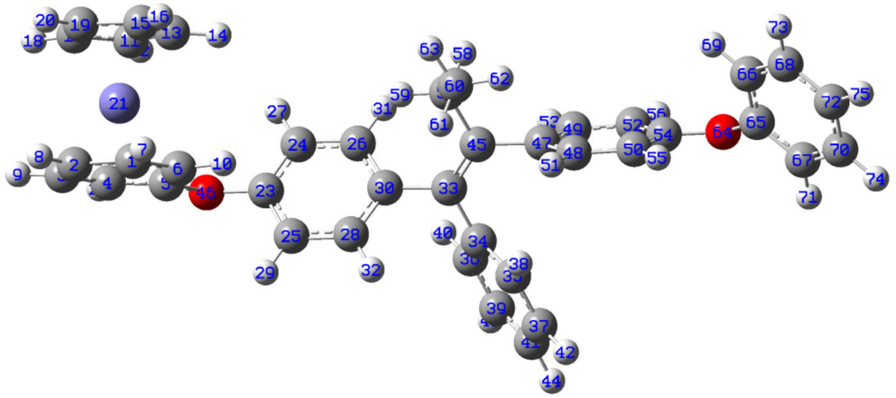

E-TPBE-Fc-1

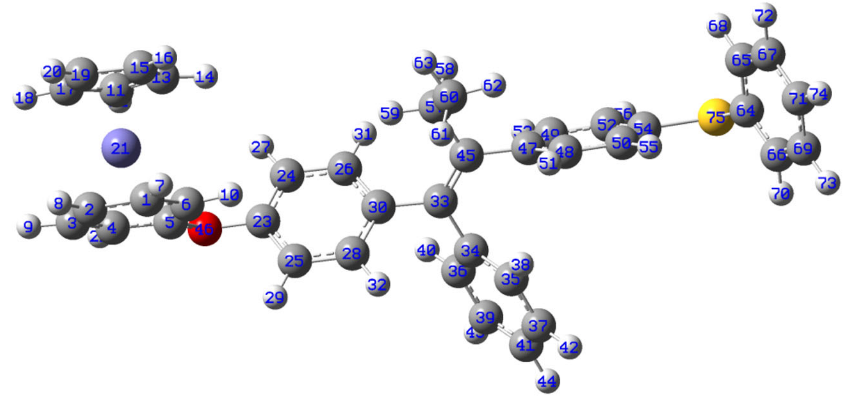

E-TPBE-Fc-2

Fig. 2 The optimized geometric structure of *E*-TPBE-Fc at DFT level

dihedral angle of 8.13°–8.60° in *E*-TPBE-Fc. According to Top et al., this angle was 13° for *E*-ferrocenyltamoxifen [36].

UV–visible spectra

The UV–visible absorption of TPBE-Fc in CH_3CN was investigated; the results are shown in Fig. 3a. TPBE-Fc has a wide conjugated absorption band in the UV–visible region from 220 nm to 350 nm; this is ascribed to an electron-transition process along the entire conjugate system.

The electron absorption spectra of TPBE-Fc-1 and TPBE-Fc-2 were calculated to rationalize the observed spectral properties; the results are shown in Fig. 3b. The first 100 spin-allowed singlet–singlet excitations for TPBE-Fc were calculated by use of the TD-DFT approach. TD-DFT calculations started from the optimized

Table 1 Selected bond distances, bond angles, and torsional angles of optimized structures of TPBE-Fc-1 and TPBE-Fc-2

Property	TPBE-Fc-1	TPBE-Fc-2	Experimental XRD[a] results of tamoxifen
Bond lengths (Å)			
C(5)–O(46)	1.338	1.338	
C(23)–O(46)	1.414	1.414	
C(33)–C(45)	1.359	1.358	1.330
Bond angles (°)			
C(5)–O(46)–C(23)	120.5	120.6	
C(30)–C(33)–C(45)	123.0	123.0	122–124
C(34)–C(33)–C(45)	123.3	123.3	122–124
C(33)–C(45)–C(57)	123.4	123.5	122–124
C(33)–C(45)–C(47)	121.0	121.1	122–124
C(54)–O(64)–C(65)	120.8		
C(54)–S(75)–C(64)		121.1	
Dihedral angles (°)			
C(30)–C(33)–C(45)–C(47)	8.16	8.13	13
C(34)–C(33)–C(45)–C(47)	8.57	8.60	

[a] From Ref. [36]

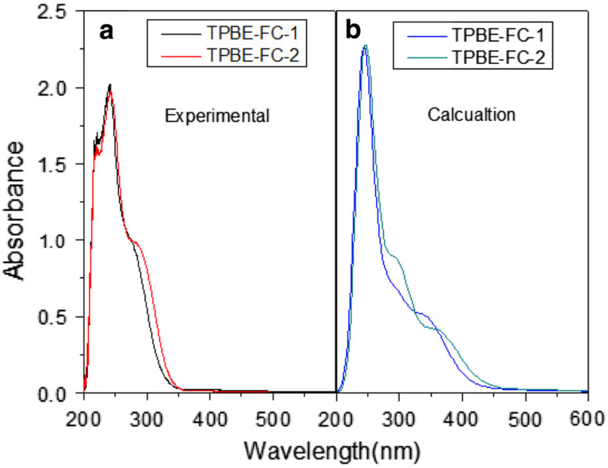

Fig. 3 Comparison of experimental (**a**) and calculated (**b**) UV–visible spectra

geometry, using the same level of theory, and were performed for the gas phase to calculate excitation energies. The wavelength (λ), oscillator strength (f_{os}), and major contributions of the calculated transitions are listed in Table 2. The calculated results are indicative of a metal-to-ligand charge transfer (MLCT) transition for TPBE-Fc and agree reasonably well with the experimentally measured spectral data

Table 2 Main electronic transitions of TPBE-Fc-1 and TPBE-Fc-2 by the TD-DFT method

Molecule	*E* (eV)	λ (nm)	f_{os}	Main contribution	Transition
TPBE-Fc-1	3.5811	346.22	0.1235	HOMO − 1 → LUMO + 4	MLCT
	5.1363	241.39	0.4291	HOMO → LUMO + 4	π–π*
				HOMO − 6 → LUMO + 4	
				HOMO − 5 → LUMO + 8	
				HOMO − 3 → LUMO + 8	
				HOMO − 2 → LUMO + 8	
				HOMO − 1 → LUMO + 8	
				HOMO − 1 → LUMO + 13	
				HOMO → LUMO + 14	
				HOMO → LUMO + 15	
TPBE-Fc-2	3.4103	363.56	0.0733	HOMO − 6 → LUMO	MLCT
	5.0858	243.79	0.4125	HOMO → LUMO + 4	π–π*
				HOMO − 6 → LUMO + 4	
				HOMO − 5 → LUMO + 8	
				HOMO − 4 → LUMO + 8	
				HOMO − 2 → LUMO + 14	
				HOMO − 1 → LUMO + 16	
				HOMO − 1 → LUMO + 17	

MLCT metal-to-ligand charge transfer

listed in Table 3. For example, the calculated gas-phase transitions for TPBE-Fc-1 and TPBE-Fc-2 appeared at 241.4 nm and 243.8 nm, in good agreement with the experimental data obtained from the UV–visible result, viz. 240 nm and 242 nm in acetonitrile solution. The value of calculated λ_{max} for TPBE-Fc-1 was blue shifted relative to that for TPBE-Fc-2, also in good agreement with the previous experimental result. MLCT of the two compounds were observed at 346.2 nm and 363.6 nm.

The UV–visible absorption spectra of TPBE-Fc in solvents of different polarity were investigated; the results are summarized in Table 3 and Fig. 4. Positive solvatochromism (bathochromic shift) of the absorption of TPBE-Fc-1 and TPBE-Fc-2 was observed on increasing the polarity of the solvent. This is related to greater stabilization of the excited state relative to the ground state with increasing solvent polarity.

HOMO and LUMO analysis

The energies of the highest occupied molecular orbital (HOMO) and the lowest unoccupied molecular orbital (LUMO) of the target compounds were computed on the basis of the optimized structures. Table 4 shows that the HOMO–LUMO energy gaps, ΔE, are smaller for TPBE-Fc than for TPBE, and that ΔE for the *E* isomers are lower than those for the *Z* isomers. Figure 5 shows the delocalization of the electron

Table 3 UV–visible data for TPBE-Fc in different solvents

Solvent	$\lambda_{\max}$ (nm)	$\varepsilon \times 10^4$ (L mol^{-1} cm^{-1})
TPBE-Fc-1		
DMF	266	0.96
THF	250	1.40
$CHCl_3$	243	1.85
CH_2Cl_2	240	1.71
CH_3CN	240	2.01
TPBE-Fc-2		
DMF	265	0.99
THF	251	1.38
$CHCl_3$	244	1.54
CH_2Cl_2	243	1.92
CH_3CN	242	1.97

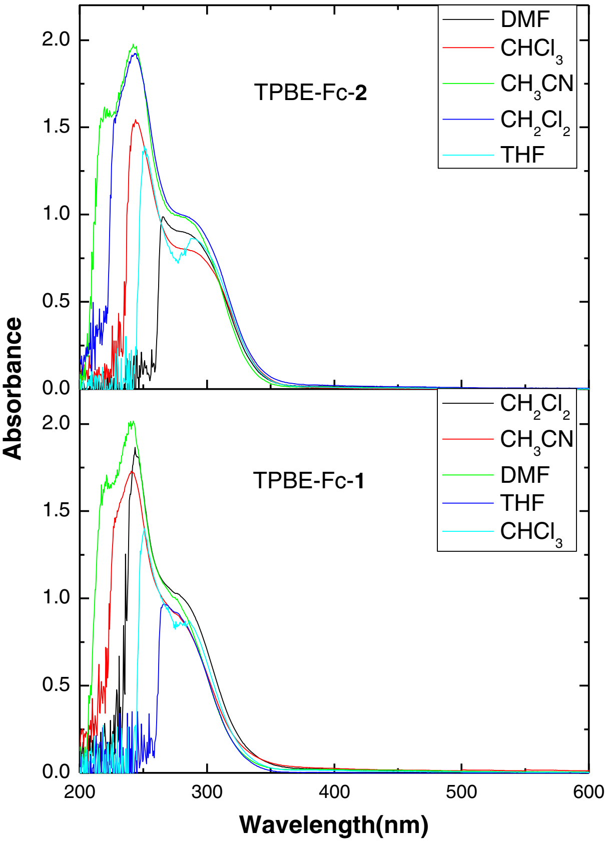

Fig. 4 UV–visible absorption spectra of TPBE-Fc in solvents of different polarity

Table 4 Calculated values of HOMO and LUMO energies and electrostatic first hyperpolarizability

Compound		E_{HOMO} (eV)	E_{LUMO} (eV)	ΔE (eV)[a]	$\beta \times 10^{-30}$ esu
TPBE-1	(*Z*)	−3.327	1.371	4.699	0.633
	(*E*)	−3.558	1.672	5.230	1.428
TPBE-2	(*Z*)	−3.177	1.379	9.327	0.810
	(*E*)	−3.281	1.690	4.970	0.729
TPBE-Fc-1	(*Z*)	−7.913	−4.950	2.963	4.216
	(*E*)	−7.171	−5.164	2.007	14.801
TPBE-Fc-2	(*Z*)	−7.790	−4.944	2.846	4.410
	(*E*)	−6.970	−5.159	1.811	16.171

[a] $\Delta E = (E_{\mathrm{LUMO}} - E_{\mathrm{HOMO}})$

densities of the frontier orbitals of the *E*-TPBE and *E*-TPBE-Fc molecules. In the HOMO and LUMO of TPBE, the electron densities are all delocalized over the –C=C– and aryl rings. From HOMO to LUMO, no electron transfer occurred in TPBE. In the HOMO of TPBE-Fc, the electron densities delocalized over the –C=C– bond and aryl rings, whereas in their LUMO orbitals the electron densities delocalized over the cyclopentadienyl iron cation and the coordinated arene. This result is clearly indicative of significant molecular charge delocalization, which strengthened its nonlinear optical (NLO) response.

Enhancement of charge separation is known to favor large NLO responses. The electrostatic first hyperpolarizability (β) was calculated by use of the Gaussian 09 package. On the basis of the calculated electronic properties and geometries, the electrostatic first hyperpolarizability β_μ was calculated by use of the DFT/B3LYP method. Values of β_μ for compounds TPBE-Fc-1 and TPBE-Fc-2 were reasonable (Table 4), although slightly weaker than values reported for the extended π-conjugated organic tolane derivative (1.02×10^{-28} esu) or the pyridoneimine derivative (2.0×10^{-29} esu) terminated with a similar cationic sandwich acceptor fragment [37]. However, the β_μ values are significantly greater than the 149, 154, and 267×10^{-48} esu values previously determined for three dipolar organoiron methylenepyran hydrazone complexes and pyranylideneacetaldehyde-hydrazone complexes with similar acceptor end groups [38, 39]. Interestingly, it is worthy of note that the second-order optical susceptibility of the target compounds followed the order: β_μ (TPBE) < β_μ (TPBE-Fc) and β_μ (*Z*) < β_μ (*E*). This trend is attributed to the intermolecular charge-transfer of the TPBE-Fc compounds. The presence of the electron-rich diphenyl ether and diphenyl sulfide moiety as a strong donor-group and the cationic cyclopentadienyliron fragment as a strong acceptor-group led to a larger value of β_μ (TPBE-Fc) than in our previous study. This switching of electron delocalization directly affected the NLO coefficient, which could generate push–pull systems. Such systems favor the generation of large NLO responses.

(*E*)-TPBE-**1 HOMO** (*E*)-TPBE-**1 LUMO**

(*E*)-TPBE-**2 HOMO** (*E*)-TPBE-**2 LUMO**

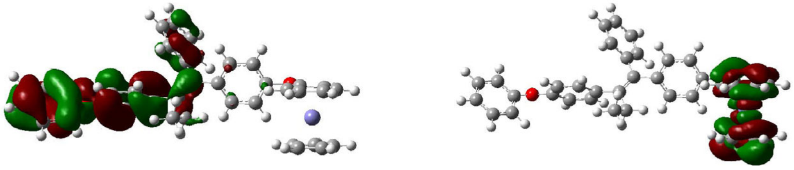

(*E*)-TPBE-Fc-**1 HOMO** (*E*)-TPBE-Fc-**1 LUMO**

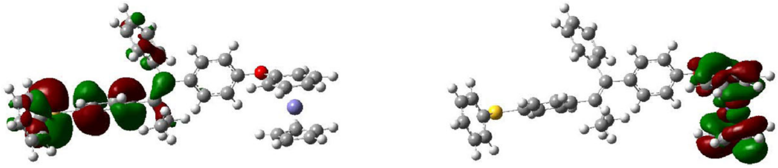

(*E*)-TPBE-Fc-**2 HOMO** (*E*)-TPBE-Fc-**2 LUMO**

Fig. 5 Molecular orbital surface and energies of the frontier molecular orbitals of *E*-TPBE and *E*-TPBE-Fc

Conclusions

In this work, two cyclopentadienyliron complexes of arene containing the triphenyl conjugated butane moiety (TPBE-Fc) were synthesized. UV–visible absorption spectra were analyzed by experimental and theoretical methods. The double bond configuration of the compounds was determined from ^{1}H NMR data. The optimized molecular structures and energy levels of frontier molecular orbitals were obtained on the basis of DFT at the B3LYP/Genecp level. It was found that these two molecules are second-order nonlinear optical materials with large first hyperpolarizability of 1.48×10^{-29} and 1.62×10^{-29} esu for *E*-TPBE-Fc-1 and *E*-TPBE-Fc-2, respectively. The cyclopentadienyl iron unit was found to be a strong electronwithdrawing group and MLCT occurs in the molecule. This change in electron distribution resulted in the high second-order optical susceptibility of TPBE-Fc.

Acknowledgments The authors wish to thank the National Natural Science Foundation of China for financial support (project grant no. 21176016). We also thank Beijing University of Chemical Technology Chem Density Computing Platform for supporting the calculations.

References

1. M. Marcaccio, J.A. McCleverty, W. Akemann, C. Fiorini-Debuisschert, J.-M. Nunzi, J. Photochem. Photobiol. A **163**, 413 (2004)
2. D. Avc, Spectrochim. Acta. A **82**, 37 (2011)
3. J. Tanihara, K. Ogawa, Y. Kobuke, J. Photochem. Photobiol. A **178**, 140 (2006)
4. X.X. Sun, G.C. Yang, S.L. Sun, N.N. Ma, Y.Q. Qiu, J. Organomet. Chem. **696**, 3384 (2011)
5. I.I. Grinval'd, A.N. Artemov, I.V. Bodrikov, L.I. Bazhan, I.Y. Kalagaev, Russ. J. Gen. Chem. **79**, 1487 (2009)
6. Y.Q. Qiu, C.S. Qin, Z.M. Su, G.C. Yang, X.M. Pan, R.S. Wang, Synth. Met. **152**, 273 (2005)
7. S. Gauthier, J. Mailhot, F. Labrie, J. Org. Chem. **61**, 3890 (1996)
8. H. Häckl, B. Behnisch, M. Hanack, Synth. Met. **121**, 1639 (2001)
9. Y. Sakai, M. Ueda, A. Yahagi, N. Tanno, Polymer **43**, 3497 (2002)
10. C. Samyn, T. Verbiest, E. Kesters, K. Van den Broeck, M. Van Beylen, A. Persoons, Polymer **41**, 6049 (2000)
11. D. Ilieva, L. Nedelchev, T. Petrova, V. Dragostinova, T. Todorov, L. Nikolova, P.S. Ramanujam, J. Opt. A **8**, 221 (2006)
12. Y.C. Zhu, D.H. He, Z.R. Yang, Spectrochim. Acta A **72**, 417 (2009)
13. J. Bao, P.M. Weber, J. Am. Chem. Soc. **133**, 4164 (2011)
14. Q. Zhang, L. Jiao, C. Shan, G. Yang, X. Xu, L. Niu, Synth. Met. **159**, 1422 (2009)
15. A. El-Wareth Sarhan, T. Izumi, Synth. Met. **140**, 95 (2004)
16. T. He, C. Wang, X. Pan, H. Yang, G. Lu, Dyes Pigm. **82**, 47 (2009)
17. M. Şenel, Synth. Met. **161**, 1861 (2011)
18. R.D.A. Hudson, I. Asselberghs, K. Clays, L.P. Cuffe, J.F. Gallagher, A.R. Manning, A. Persoons, K. Wostyn, J. Organomet. Chem. **637**, 435 (2001)
19. K.R.J. Thomas, J.T. Lin, Y.S. Wen, J. Organomet. Chem. **575**, 301 (1999)
20. S. Top, A. Vessières, C. Cabestaing, I. Laios, G. Leclercq, C. Provot, G. Jaouen, J. Organomet. Chem. **637**, 500 (2001)
21. R.J. Han, G.L. Li, T. Wang, Inorg. Chim. Acta **392**, 374 (2012)
22. N. Nesmeyanov, N.A. Vol'kenau, I.N. Bolesova, Dolk. Akad. Nauk S.S.S.R. **149**, 615 (1963). (English translation p. 267–268)
23. A.N. Nesmeyanov, N.A. Vol'kenau, I.N. Bolesova, Tetrahedron Lett. **25**, 1725 (1963)
24. P.J. Stephens, F.J. Devlin, C.F. Chabalowski, M.J. Frisch, J. Phys. Chem. **98**, 11623 (1994)
25. A.D. Becke, Phys. Rev. A **38**, 3098 (1988)
26. P.J. Hay, W.R. Wadt, J. Chem. Phys. **82**, 270 (1985)
27. M.M. Frand, W.J. Pietro, W.J. Hehre, J.S. Binkley, D.J. DeFrees, J.A. Pople, M.S. Gordon, J. Chem. Phys. **77**, 3654 (1982)
28. P.C. Hariharan, J.A. Pople, Theor. Chem. ACC **28**, 213 (1973)
29. M.J. Frisch, G.W. Trucks, H.B. Schlegel, G.E. Scuseria, M.A. Robb, J.R. Cheeseman, G. Scalmani, V. Barone, B. Mennucci, G.A. Petersson, Gaussian 09, Revision A **02** (2009)
30. M.K. Casida, C. Jamorski, K.C. Casida, D.R. Salahub, J. Chem. Phys. **108**, 4439 (1998)
31. R.E. Stratmann, G.E. Scuseria, J. Chem. Phys. **109**, 8218 (1998)
32. P.S. Liyanage, R.M. de Silva, K.M. Nalin de Silva, J. Mol. Struct. Theochem. **639**, 195 (2003)
33. N.N. Ma, G.C. Yang, S.L. Sun, C.G. Liu, Y.Q. Qiu, J. Organomet. Chem. **696**, 2380 (2011)
34. D.J. Collins, J.J. Hobbs, C.W. Emmens, J. Med. Chem. **14**, 953 (1971)
35. J. Gilbert, J.F. Miquel, G. Precigoux, M. Hospital, J.P. Raynaud, F. Michel, A. Crastes de Paulet, J. Med. Chem. **26**, 693 (1983)
36. S. Top, A. Vessières, G. Leclercq, J. Quivy, J. Tang, J. Vaissermann, M. Huché, G. Jaouen, Chem. Eur. J. **9**, 5223 (2003)

37. C. Lambert, W. Gaschler, M. Zabel, R. Matschiner, R. Wortmann, J. Organomet. Chem. **592**, 109 (1999)
38. L. Millan, M. Fuentealba, C. Manzur, D. Carrillo, N. Faux, B. Caro, F.R. Guen, S. Sinbandhit, I. Ledoux-Rak, J.R. Hamon, Eur. J. Inorg. Chem. **2006**, 1131 (2006)
39. M. Fuentealba, L. Toupet, C. Manzur, D. Carrillo, I. Ledoux-Rax, J.R. Hamon, J. Organomet. Chem. **692**, 1099 (2007)